

# Taming Food–Drug Interaction Risk: Potential Inhibitory Effects of Citrus Juices on Cytochrome Liver Enzymes Can Safeguard the Liver from Overdose Paracetamol-Induced Hepatotoxicity

Aya S. Shalaby,\* Hanaa H. Eid, Riham A. El-Shiekh, Osama G. Mohamed, Ashootosh Tripathi, Ahmed A. Al-Karmalawy, Amany A. Sleem, Fatma Adly Morsy, Khaled M. Ibrahim, Soad H. Tadros, and Fadia S. Youssef

Cite This: *ACS Omega* 2023, 8, 26444–26457

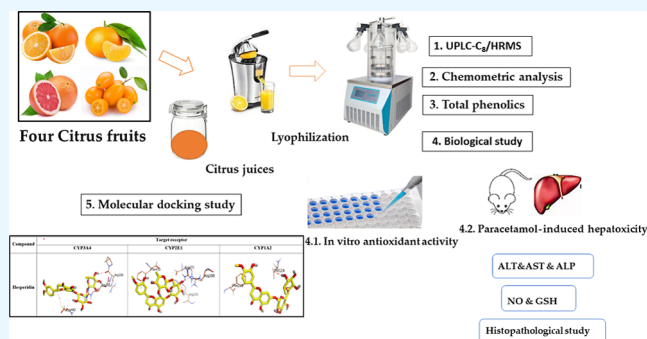
Read Online

ACCESS |

Metrics & More

Article Recommendations

**ABSTRACT:** Paracetamol overdose is the leading cause of drug-induced hepatotoxicity worldwide. Because of *N*-acetyl cysteine's limited therapeutic efficacy and safety, searching for alternative therapeutic substitutes is necessary. This study investigated four citrus juices: *Citrus sinensis* L. Osbeck var. Pineapple (pineapple sweet orange), *Citrus reticulata* Blanco × *Citrus sinensis* L. Osbeck (Murcott mandarin), *Citrus paradisi* Macfadyen var. Ruby Red (red grapefruit), and *Fortunella margarita* Swingle (oval kumquat) to improve the herbal therapy against paracetamol-induced liver toxicity. UHPLC-QTOF-MS/MS profiling of the investigated samples resulted in the identification of about 40 metabolites belonging to different phytochemical classes. Phenolic compounds were the most abundant, with the total content ranked from 609.18 to 1093.26  $\mu\text{g}$  gallic acid equivalent (GAE)/mL juice. The multivariate data analysis revealed that phloretin 3',5'-di-*C*-glucoside, narirutin, naringin, hesperidin, 2-*O*-rhamnosyl-swertisin, fortunellin (acacetin-7-*O*-neohesperidoside), sinensetin, nobiletin, and tangeretin represented the crucial discriminatory metabolites that segregated the analyzed samples. Nevertheless, the antioxidant activity of the samples was 1135.91–2913.92  $\mu\text{M}$  Trolox eq/mL juice, 718.95–3749.47  $\mu\text{M}$  Trolox eq/mL juice, and 2304.74–4390.32  $\mu\text{M}$  Trolox eq/mL juice, as revealed from 2,2'-azino-bis-3-ethylbenzthiazoline-6-sulfonic acid, ferric-reducing antioxidant power, and oxygen radical absorbance capacity, respectively. The *in vivo* paracetamol-induced hepatotoxicity model in rats was established and assessed by measuring the levels of hepatic enzymes and antioxidant biomarkers. Interestingly, the concomitant administration of citrus juices with a toxic dose of paracetamol effectively recovered the liver injury, as confirmed by normal sections of hepatocytes. This action could be due to the interactions between the major identified metabolites (hesperidin, hesperetin, phloretin 3',5'-di-*C*-glucoside, fortunellin, poncirin, nobiletin, apigenin-6,8-digalactoside, 6',7'-dihydroxybergamottin, naringenin, and naringin) and cytochrome P450 isoforms (CYP3A4, CYP2E1, and CYP1A2), as revealed from the molecular docking study. The most promising compounds in the three docking processes were hesperidin, fortunellin, poncirin, and naringin. Finally, a desirable food–drug interaction was achieved in our research to overcome paracetamol overdose-induced hepatotoxicity.



## 1. INTRODUCTION

Paracetamol is a highly efficient and extensively used analgesic and antipyretic worldwide.<sup>1</sup> Despite its therapeutic value, paracetamol-induced hepatotoxicity is one of the most pervasive types of poisoning globally.<sup>2</sup> The perspective of paracetamol as a safe over-the-counter medication has already become totally ambiguous, resulting in a significantly high rate of hepatic injury and even death. That may occur at doses just slightly higher than the maximum therapeutic dose, which is stated by the Food and Drug Administration (FDA) of the United States as 4000 mg of acetaminophen per day.<sup>3</sup> According to the Poison Control Center at Ain Shams University Hospitals (PCC-ASUH), which

is considered Egypt's primary poison control center, "Paracetamol ranks among the top 10 exposure substances that PCC-ASUH received the most in 2019".<sup>4</sup>

The WHO<sup>5</sup> urged people on March 17, 2020, with coronavirus disease 2019 (COVID-19) symptoms to avoid

Received: May 5, 2023  
Accepted: June 30, 2023  
Published: July 17, 2023



Table 1. Metabolites Tentatively Identified in Citrus Juices Using UPLC-MS/MS<sup>a</sup>

No.	Rt.	chemical classes	Tentatively Identified Compounds	Molecular Formula	[M+H] <sup>+</sup>	Fragments (+)	[M-H] <sup>-</sup>	Fragments (-)	OP	OPA	OF	MP	MPA	MF	GP	GPA	GF	KP	KPA	KF	Ref.	
1	0.41	amino acid	Arginine	C <sub>6</sub> H <sub>14</sub> N <sub>4</sub> O <sub>2</sub>	175.1184	158.0322, 130.0981, 116.0714, <b>70.0657</b> , 60.0563	-	-	+	+	+	+	+	+	+	+	+	+	+	+	[28]	
2	0.46	carbohydrate	Sucrose	C <sub>12</sub> H <sub>22</sub> O <sub>11</sub>	365.1061 (M+Na) <sup>+</sup>	365.1039, 247.0337, 229.0957, <b>203.0520</b> , 185.0417	-	-	+	+	+	+	+	+	+	+	+	+	+	+	[29]	
3	0.47	organic acid	Citric acid	C <sub>6</sub> H <sub>8</sub> O <sub>7</sub>	-	-	191.0198	191.0546, 129.0193, 111.0079, <b>87.0081</b> , 57.0343	+	+	+	+	+	+	+	+	+	+	+	+	[30]	
4	0.74	amino acid glucoside	Tryptophan N-glucoside	C <sub>17</sub> H <sub>22</sub> N <sub>2</sub> O <sub>7</sub>	367.1501	332.1117, 205.0614, <b>188.0709</b> ,	-	-	-	+	-	+	+	+	+	+	+	+	-	-	[31]	
5	0.82	amino acid	L-Tryptophan	C <sub>11</sub> H <sub>12</sub> N <sub>2</sub> O <sub>2</sub>	205.0907	188.0708, 170.0593, 143.0720, 146.0593, <b>118.0646</b> , 91.0544	-	-	-	-	-	-	-	+	-	+	+	-	-	-	[32]	
6	1.04	phenolic acid	Feruloyl putrescine	C <sub>14</sub> H <sub>20</sub> N <sub>2</sub> O <sub>5</sub>	265.1551	<b>177.0546</b> , 144.1029	-	-	+	+	+	-	-	-	+	+	+	-	-	-	[33]	
7	1.11	phenolic glycoside	Syringin	C <sub>17</sub> H <sub>22</sub> O <sub>9</sub>	395.1315 (M+Na) <sup>+</sup>	365.1054, <b>233.0744</b> , 185.0422	-	-	+	+	+	+	+	+	-	+	+	-	+	+	[34]	
8	1.71	phenolic acid	Ferulic acid	C <sub>10</sub> H <sub>10</sub> O <sub>4</sub>	177.055 (M-H <sub>2</sub> O+H) <sup>+</sup>	177.0330, 149.0589, 145.0278, 134.0351, 106.0408, 91.0536, 89.0383, 77.0383	-	-	+	+	+	+	+	+	+	+	+	-	-	-	[35]	
9	1.76	flavone glycoside	Luteolin C-glucoside-arabinoside	C <sub>27</sub> H <sub>30</sub> O <sub>16</sub>	611.1613		-	-	-	+	+	-	-	+	-	-	-	-	-	-	[36]	
10	1.84	phenolic acid	Sinapic acid	C <sub>11</sub> H <sub>12</sub> O <sub>5</sub>	225.0655	192.0419, 177.0538, 175.0409, 164.0473, 147.0455, 132.0207, <b>119.0496</b> , 91.0549, 65.0394	-	-	-	+	-	-	+	+	+	+	+	-	-	+	[35]	
11	1.84	phenolic glycoside	Iriflophenone glycoside	C <sub>19</sub> H <sub>20</sub> O <sub>10</sub>	409.111		-	-	+	+	+	+	+	+	-	+	+	+	+	+	[36]	
12	2.22	flavone glycoside	apigenin 6,8-digalactoside	C <sub>27</sub> H <sub>30</sub> O <sub>15</sub>	595.1669		593.1522		+	+	+	+	+	+	+	+	+	+	-	+	[36]	
13	2.54	flavone glycoside	Isovitexin 2''-O-rhamnoside	C <sub>27</sub> H <sub>30</sub> O <sub>14</sub>	-	-	577.1574	413.0888, 341.0681, 311.0576, <b>293.0471</b>	-	-	-	-	-	+	-	+	+	+	-	-	[37]	
14	2.64	flavone glycoside	Isovitexin O-arabinoside	C <sub>26</sub> H <sub>28</sub> O <sub>14</sub>	565.1558	433.1121, 415.1024, 337.0702, <b>313.0702</b> , 283.0597	563.1414	443.0988, 413.0863, <b>293.0455</b> , 164.1540	-	+	+	-	+	+	+	+	+	+	-	-	-	[38]
15	2.72	flavonol glycoside	Rutin	C <sub>27</sub> H <sub>30</sub> O <sub>17</sub>	-	-	609.1418	463.1246, 301.0350, <b>300.0280</b> , 271.0239	-	+	+	-	-	+	-	-	-	-	-	-	[39]	
16	2.74	flavanone glycoside	Narirutin	C <sub>27</sub> H <sub>32</sub> O <sub>14</sub>	581.1867	<b>581.1807</b> , 419.1241, 273.0636, 174.9891, 153.0064	-	-	-	+	+	+	+	+	+	+	+	+	+	+	[40]	
17	2.74	chalcone glycoside	Di-C-β-glucopyranosyl phloretin (DGPP)	C <sub>27</sub> H <sub>34</sub> O <sub>15</sub>	599.198	<b>593.1874</b> , 581.1868, 479.1557, 461.1452, 437.1421, 359.1140	-	-	-	-	-	-	-	-	-	-	-	+	+	+	[41]	
18	2.74	flavone glycoside	Isoswertisin O-glucoside	C <sub>28</sub> H <sub>32</sub> O <sub>15</sub>	609.1823		-	-	-	-	-	-	-	-	-	-	-	-	+	+	[36]	
19	2.83	flavone glycoside	Kaempferol O-rutinose	C <sub>27</sub> H <sub>30</sub> O <sub>15</sub>	595.1676	471.2034, 393.1900, 343.1748, <b>287.0427</b> , 273.0758, 153.0046, 117.0338, 85.0174	-	-	-	-	+	-	-	+	-	+	-	-	-	-	[30, 35]	
20	2.91	flavone glycoside	Isorhamnetin O-rutinose	C <sub>28</sub> H <sub>32</sub> O <sub>16</sub>	-	-	623.1625	623.1591, <b>315.0513</b> , 300.0280, 299.0197	-	+	+	-	+	+	-	-	-	-	-	-	[30]	
21	2.96	flavanone glycoside	Naringin	C <sub>27</sub> H <sub>32</sub> O <sub>14</sub>	581.1867	<b>273.0762</b> , 153.0187, 147.0441, 129.0551	-	-	-	+	+	+	+	+	+	+	+	-	-	-	[28]	
22	3.01	flavone glycoside	Rhoifolin	C <sub>27</sub> H <sub>30</sub> O <sub>14</sub>	579.1708	433.1360, 336.1718, <b>271.0605</b> , 153.0189, 85.0283	577.1579	<b>269.0463</b>	-	-	-	-	-	+	-	+	+	+	+	+	[35, 42]	
23	3.06	flavanone glycoside	Hesperidin	C <sub>28</sub> H <sub>34</sub> O <sub>15</sub>	611.1986	449.1468, <b>303.0884</b> , 263.0560, 245.0449, 219.0313, 195.0304, 177.0562, 165.0186, 153.0190, 129.0551, 85.0289	609.1835		+	+	+	+	+	+	+	+	+	-	-	-	[35, 40]	
24	3.07	flavonol glycoside	Quercitrin	C <sub>21</sub> H <sub>22</sub> O <sub>11</sub>	449.1439	<b>303.0839</b> , 219.0272, 165.0176, 153.0170, 135.0430	-	-	+	+	+	-	+	+	-	+	+	-	-	-	[43, 44]	
25	3.16	flavone glycoside	O-rhamnosyl-swertisin	C <sub>28</sub> H <sub>32</sub> O <sub>14</sub>	593.1877	447.1285, 429.1179, 411.1078, 351.0862, <b>327.0866</b> , 297.0756, 285.0799	-	-	-	-	-	-	-	-	-	-	-	+	+	+	[45]	
26	3.19	coumarin	Scoparone	C <sub>10</sub> H <sub>10</sub> O <sub>4</sub>	207.0657	<b>207.0657</b> , 191.0339, 163.0393, 151.0757, 136.0519	-	-	-	+	+	-	+	+	-	-	-	-	-	-	[46]	
27	3.44	flavone glycoside	Fortunellin	C <sub>28</sub> H <sub>32</sub> O <sub>14</sub>	593.1872	<b>285.0778</b>	-	-	-	-	-	-	-	-	-	-	-	+	+	+	[47]	
28	3.46	flavanone glycoside	Isosakuranetin O-rutinose (didymin)	C <sub>28</sub> H <sub>34</sub> O <sub>14</sub>	-	-	639.1942 (M+FA-H) <sup>-</sup>	593.1893, 473.0472, 327.0883, <b>285.0778</b> , 164.0114, 151.0043	-	+	+	+	+	+	+	+	+	-	-	-	[48]	

Table 1. continued

29	3.47	flavone glycoside	Poncirin		617.1837 (M+Na) <sup>+</sup>	595.2001, 433.1476, 331.0984, 287.0902, 153.0179	-	-	-	+	+	+	+	+	+	+	+	+	+	+	[28]
30	3.91	coumarin	Umbelliferone	C <sub>9</sub> H <sub>6</sub> O <sub>3</sub>	163.0393	119.0491, 107.0491, 77.0384	-	-	-	-	-	-	-	-	+	+	+	-	-	-	[49]
31	4.22	furanocoumarin	Dihydroxybergamottin	C <sub>12</sub> H <sub>12</sub> O <sub>6</sub>	395.1474 (M+Na) <sup>+</sup>	355.1543, 337.1452, 203.0345, 153.1280	-	-	-	-	-	-	-	-	+	+	+	-	-	-	[50]
32	4.24	flavone	Sinensetin	C <sub>20</sub> H <sub>20</sub> O <sub>7</sub>	373.1176	358.1053, 343.0820, 312.0998, 297.0758, 151.0391	-	-	-	+	+	+	+	+	-	+	+	-	-	-	[40]
33	4.29	flavone	Demethoxytangeretin	C <sub>19</sub> H <sub>18</sub> O <sub>6</sub>	343.1176	328.0943, 313.0708, 285.0757, 181.0129	-	-	-	-	-	-	+	+	-	-	+	-	-	-	[51]
34	4.43	flavone	Nobiletin	C <sub>21</sub> H <sub>22</sub> O <sub>8</sub>	403.1396	388.1134, 373.0951, 355.0797, 327.0849, 211.0230	-	-	+	+	+	+	+	+	-	+	+	-	-	-	[35, 40]
35	4.47	triterpenoid	Limonin	C <sub>28</sub> H <sub>30</sub> O <sub>8</sub>	471.2021	425.1938, 279.1352, 213.0902, 161.0599, 105.0693, 95.0125	469.187	454.9678, 411.1427, 367.1879, 229.1226, 191.3026	+	+	+	+	+	+	+	+	+	-	-	-	[40, 52]
36	4.49	flavone	Artemetin	C <sub>20</sub> H <sub>20</sub> O <sub>8</sub>	389.1223	374.0984, 356.0871, 331.0804, 313.0690	-	-	-	-	+	-	-	-	-	-	-	-	-	-	[53, 54]
37	4.55	flavone	Methoxynobiletin	C <sub>22</sub> H <sub>22</sub> O <sub>10</sub>	433.1499	418.1268, 403.1394, 385.0924, 357.0973, 343.1187	-	-	+	+	+	+	+	+	-	+	+	-	-	-	[40]
38	4.66	flavone	Tangeretin	C <sub>20</sub> H <sub>20</sub> O <sub>7</sub>	373.1288	358.1068, 343.0833, 325.0723, 297.0771	-	-	-	+	+	+	+	+	-	+	+	-	-	-	[40]
39	4.68	triterpenoid	Nomilin	C <sub>28</sub> H <sub>34</sub> O <sub>9</sub>	515.2294	469.2241, 369.2054, 343.1327, 205.0498, 161.0604, 133.0660, 105.0709, 81.0340	-	-	+	+	+	+	+	+	-	-	+	-	-	-	[35]
40	4.88	flavone	O-Demethylnobiletin	C <sub>20</sub> H <sub>20</sub> O <sub>8</sub>	389.1234	374.1003, 359.0786, 341.0672, 328.0951, 274.2739, 214.0389, 165.0557, 124.0863	-	-	-	-	+	-	-	+	-	+	-	-	-	-	[35, 40]

<sup>a</sup>OP; pineapple orange with pulp, OPA; pineapple orange with pulp and albedo, OF; pineapple orange whole fruit, MP; Murcott mandarin with pulp, MPA; Murcott mandarin with pulp and albedo, MF; Murcott mandarin whole fruit, GP; red grapefruit with pulp, GPA; red grapefruit with pulp and albedo, GF; red grapefruit whole fruit, KP; oval kumquat with pulp, KPA; oval kumquat with pulp and albedo, KF; oval kumquat whole fruit, (+); present, (-); absent.

ibuprofen and instead utilize paracetamol.<sup>6</sup> Moreover, paracetamol has been considered the first choice analgesic and antipyretic used for COVID-19 patients considering the WHO pain management ladder.<sup>7</sup> Consequently, these concerns have intensified during the COVID-19 pandemic because of the exceptionally excessive purchase and domiciliary use without considering the safety measures.<sup>8</sup>

After a paracetamol overdose, cytochrome P450 isoenzymes bioactivate the excess paracetamol to a hepatotoxic metabolite, *N*-acetyl-*p*-benzoquinoneimine (NAPQI).<sup>9</sup> *N*-acetyl cysteine is considered the drug of choice as the treatment in cases of paracetamol overdose.<sup>10</sup> However, its utilization is hindered by disability to stop the NAPQI formation, besides the panic of its hypersensitivity.<sup>11</sup>

CYP3A4 is a drug-metabolizing enzyme of the P450 superfamily that is abundantly expressed in the human liver and plays a significant role in drug metabolism.<sup>12,13</sup> Furthermore, previous studies reported that administering a hepatotoxic dose of paracetamol combined with known inhibitors of CYP 3A4, 2E1, and 1A2, for instance, isoniazid, caffeine, and ketoconazole, could prevent the progression of paracetamol-induced hepatotoxicity.<sup>14</sup> Unfortunately, these medications were unable to be further investigated because of their side effects and therapeutic use.

As traditional herbal medicines are widely applied, herb–drug interactions have become an increasing issue in the clinical use of conventional drugs. Herb–drug interactions can have a variety of outcomes: on the one hand, they can affect drug levels and/or activities, potentially leading to therapeutic failure or adverse reactions; on the other hand, some can result in beneficial clinical effects such as increased efficacy and decreased side effects.<sup>15</sup> As a result, it became necessary to find more safe and suitable candidates for preventing paracetamol-induced hep-

atotoxicity. It is well known that medicinal plants containing phenolics as flavonoids (e.g., citrus) have antioxidant, hepatoprotective, membrane-stabilizing activity, and CYP2E1 inhibitory effects.<sup>16</sup> Citrus plants have great importance which could be attributed to several medicinally bioactive metabolites, for example, essential oils, limonoids, furanocoumarins, flavonoids, sterols, alkaloids, and carotenoids.<sup>17</sup> In recent years, there have been reports of interactions between citrus fruit products and several drugs.<sup>18,19</sup> Notably, even just a single glass of grapefruit juice causes a marked decline in CYP3A4 substrate metabolism. When grapefruit is consumed repeatedly, hepatic CYP3A4 activity decreases.<sup>20</sup> Other citrus juices may have comparable effects *via* a different mechanism, resulting in a decrease in the systemic concentration of specific medications.<sup>21</sup>

Thus, the aim of this research was to demonstrate how the four common Egyptian citrus juices; *Citrus sinensis* L. Osbeck *var.* Pineapple (sweet orange), *Citrus reticulata* Blanco × *Citrus sinensis* L. Osbeck (Murcott mandarin), *Citrus paradisi* Macfadyen *var.* Ruby Red (red grapefruit), and *Fortunella margarita* Swingle (oval kumquat) had CYP P450 inhibition activity with an impact on the prevention of paracetamol-induced hepatotoxicity following an overdose in rats.

## 2. RESULTS

**2.1. UHPLC–MS/MS Analysis.** The retention times, identities, observed molecular weights, and fragment ions for individual metabolites are shown in Table 1. The identified metabolites belong to different classes of compounds: 25 flavonoids, 3 phenolic acids, 2 phenolic glycosides, 2 coumarins, 1 furanocoumarin, 2 triterpenoids, 2 amino acids, 1 amino acid glucoside, 1 sugar, and 1 organic acid. The mass fragmentations of identified metabolites were compared to the previous published references or database, as illustrated in Table 1.



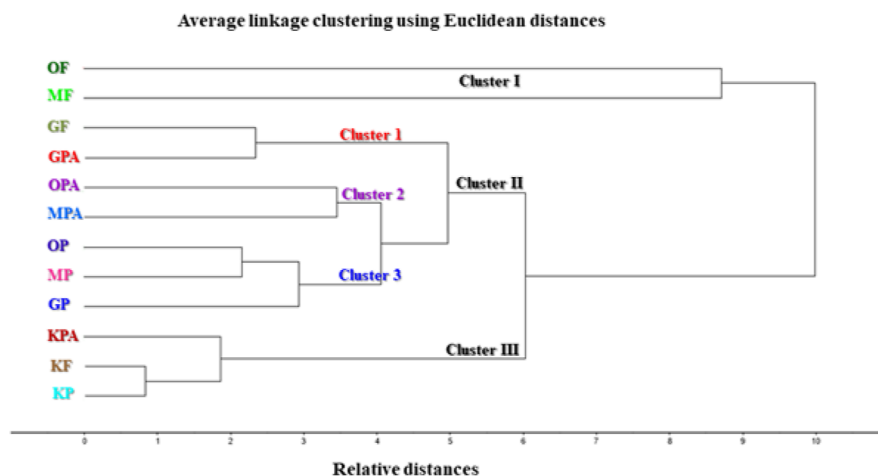


**Figure 2.** HCA dendrogram for discrimination of citrus species based upon LC/MS analyses of their juices where pineapple orange whole fruit (OF); pineapple orange with pulp and albedo (OPA); pineapple orange with pulp only (OP); Murcott mandarin whole fruit (MF); Murcott mandarin with pulp and albedo (MPA); Murcott mandarin with pulp (MP); red grapefruit whole fruit (GF); red grapefruit with pulp and albedo (GPA); red grapefruit with pulp (GP); oval kumquat whole fruit (KF); oval kumquat with pulp and albedo (KPA); oval kumquat with pulp (KP); the average of three triplicate readings.

The quantity and location of methoxy groups affect these compounds' bioavailability.<sup>23</sup>

Additionally, rutin (**compound 15**) and quercitrin (**compound 24**) were identified as flavonol glucosides.

Also, 10 flavone glycosides were identified, namely as luteolin 6-C-glucoside 8-C-arabinoside (**compound 9**), apigenin 6,8-digalactoside (**compound 12**), isovitexin 2''-O-rhamnoside (**compound 13**), isovitexin 2''-O-arabinoside (**compound 14**), isoswertisin-O-glucoside (**compound 18**), kaempferol 3-O-rutinoside (**compound 19**), isorhamnetin 3-O-rutinoside (**compound 20**), rhoifolin (**compound 22**), 2-O-rhamnosylswertisin (**compound 25**), and fortunellin (**compound 27**). Fortunellin (acacetin-7-O-neohesperidoside) has long been recognized as a significant component in kumquats.<sup>22,24</sup>

Furthermore, 3',5'-di-C- $\beta$ -glucopyranosyl phloretin (DGPP) (**compound 17**) was shown to be the identified dihydrochalcone C-glycoside in oval kumquat juices only. This is consistent with previously reported findings stating that the flavonoid DGPP is a feature of the genus *Fortunella*.<sup>25</sup>

**2.1.2. Coumarins and Furanocoumarin.** Scoparone (**compound 26**) and umbelliferone (**compound 30**) were the detected coumarins, where umbelliferone is a characteristic of grapefruits. Moreover, 6',7'-dihydroxy-bergamottin (**compound 31**) is a natural furanocoumarin found in grapefruits in both the peel and the pulp and is reported to be responsible for many grapefruit–drug interactions.<sup>26</sup>

**2.1.3. Phenolic Acids.** Feruloyl putrescine (**Compound 6**), Ferulic acid (**Compound 8**), and Sinapic acid (**Compound 10**) were identified.

**2.1.4. Phenolic Glycoside.** Syringin (**Compound 7**) and Iriflophenone 2-glucoside (**Compound 11**) were identified. These compounds were fragmented to yield free phenolic acid through bond cleavage of glycosidic linkage, followed by additional cleavage caused by the loss of carboxylic or hydroxyl groups.

**2.1.5. Triterpenoids.** Tetranortriterpenoids, known as limonoids, are among the bioactive compounds in citrus products that have the greatest health benefits. The examined samples contained limonin (**compound 35**) and nomilin (**compound 39**), which are known to be the main limonoids in citrus fruits.<sup>27</sup>

**2.1.6. Miscellaneous Compounds.** Two amino acids were identified as arginine (**compound 1**) and L-tryptophan (**compound 5**), and one organic acid was identified as citric acid (**compound 3**), in addition to one amino acid glucoside, namely, tryptophan N-glucoside, and one sugar identified as sucrose (**compound 2**).<sup>28–54</sup>

## 2.2. Metabolic Discrimination of Citrus Species Based on UPLC-MS/MS Analysis Coupled with Chemometrics.

Chemometric analysis of citrus species under investigation was done relying upon qualitative and quantitative information compiled from LC/MS study of the juices acquired from the different layers of their fruits, namely, the whole fruit, pulp and albedo, and pulp only. Twelve samples were compared using principal component analysis (PCA) and hierarchical cluster analysis (HCA) as unsupervised pattern recognition models. These samples were OP, OPA, OF, MP, MPA, MF, GP, GPA, GF, KP, KPA, and KF. The PCA score plot for principal components (PCs) extracted seven PCs, accounting for 98.47% of the total variances, whereas PC1 versus PC2 accounted for 53 and 18% of the total variance, respectively. Moreover, the PCA score plot results, presented in Figure 1A, successfully segregated the examined samples into three main clusters. OF and MF are clustered together in the left upper quadrant, showing negative values for PC1 and positive values for PC2 (cluster I). MPA, OPA, GF, GPA, MP, OP, and GP are clustered together in cluster II, which is allocated in the lower quadrants on either side of PC1, showing negative values for PC2. However, KP, KPA, and KF are gathered in cluster III on the right upper quadrant, revealing positive values for both PCs. Meanwhile, cluster II was re-clustered into three discriminant sub-clusters where MP, OP, and GP were collected in one cluster existed on the right lower quadrant, showing positive values for PC1 where negative values for PC2; GF and GPA were segregated together, whereas MPA and OPA are collected in one separate cluster. Through a comprehensive examination of the score plot, it was clearly obvious that PC1 significantly discriminates cluster I from cluster III, whereas PC2 effectively separates clusters I and III from cluster II, and this basically depends on the qualitative and quantitative variation in their predominant secondary metabolites that greatly reflected upon their biological activities. Additionally, the loading plot

displayed in Figure 1B highlighted that phloretin 3',5'-di-C-glucoside (3' 5'-di-C- $\beta$ -glucopyranosyl phloretin), naringin, naringin, hesperidin, 2-O-rhamnosyl-swertisin, fortunellin (acetin-7-O-neohesperidoside), sinensetin, nobiletin, and tangeretin represented the crucial discriminatory metabolites that caused the segregation of the analyzed samples.

Moreover, HCA was further ascertained from PCA results, where the HCA dendrogram revealed the classification of the tested samples into three main clusters: clusters I, II, and III, of which cluster II was further separated into sub-clusters 1, 2, and 3, as illustrated in Figure 2, where HCA results came in coincidence with PCA results.

**2.3. Total Phenolic Content.** Phenolics in our study of the fresh juices obtained from OP, MP, GP, and KF ranged from 609.18 to 1093.26  $\mu$ g gallic acid equivalent/mL juice (GAE/mL juice). Among juice samples, it was revealed that OP showed the highest total phenolic content (1093.26  $\pm$  39.56  $\mu$ g GAE/mL juice), followed by GP and KF (790.40  $\pm$  13.01 and 736.93  $\pm$  15.50  $\mu$ g GAE/mL juice, respectively), and the last one was MP (609.18  $\pm$  19.38  $\mu$ g GAE/mL juice).

**2.4. In Vitro Assessment of Antioxidant Capacity.** The antiradical, ferric ion-reducing power, and reactive oxygen species (ROS) scavenging activities were estimated using ABTS, FRAP, and ORAC, respectively. All the tested juices revealed antioxidant potency throughout those three different assays, as represented in Table 2. The results were expressed as  $\mu$ M Trolox

**Table 2. In Vitro Antioxidant Activity of the Investigated Citrus Juices<sup>a</sup>**

Citrus juice sample	ABTS	FRAP	ORAC
OP	2913.92 $\pm$ 134.12	3749.47 $\pm$ 87.55	4390.32 $\pm$ 161.57
MP	1135.91 $\pm$ 58.49	997.89 $\pm$ 85.19	2304.74 $\pm$ 323.37
GP	1838.61 $\pm$ 83.27	2229.47 $\pm$ 46.78	3737.17 $\pm$ 434.20
KF	2691.25 $\pm$ 67.67	718.95 $\pm$ 49.65	3689.22 $\pm$ 197.86

<sup>a</sup>OP; pineapple orange pulp juice, MP; Murcott mandarin pulp juice, GP; red grapefruit pulp juice, KF; oval kumquat whole fruit juice, ABTS; 2,2'-azino-bis (3-ethylbenzothiazoline-6-sulfonic acid), FRAP; ferric-reducing antioxidant power, ORAC; oxygen radical absorbance capacity. The results were expressed as  $\mu$ M Trolox eq/mL juice  $\pm$  SD.

equivalent per mL of juice. The samples showed antioxidant values ranging from 1135.91 to 2913.92  $\mu$ M Trolox eq/mL juice, 718.95 to 3749.47  $\mu$ M Trolox eq/mL juice, and 2304.74 to 4390.32  $\mu$ M Trolox eq/mL juice in ABTS, FRAP, and ORAC, respectively.

**2.5. In Vivo Assessment of the Interactions of Citrus Juices in Case of Paracetamol Overdose-Induced Hepatotoxicity.** From our results (Table 3), alanine transaminase (ALT), aspartate transaminase (AST), and alkaline phosphatase (ALP) levels were switched after paracetamol overdose from 32.36 to 149.57 U/L, 53.43 to 237.68 U/L, and 116.42 to 321.43 U/L, respectively, indicating increments of 4.62, 4.44, and 2.76 folds. The level of nitric oxide (NO) also was turned from 19.31 to 63.37  $\mu$ mol/g tissue (3.28-fold increment than the normal level), in addition to glutathione reductase (GSH) that dropped from 8.67 to 3.21  $\mu$ mol/g tissue (2.7-fold reduction from normal values). In contrast, administration of silymarin enhanced the values of ALT, AST, ALP, NO, and GSH by (percentage change)  $-67.43$ ,  $-71.65$ ,  $-59.13$ ,  $-66.66$ , and  $144.86\%$  compared to the paracetamol-treated group, respectively. Noteworthy, when paracetamol was simultaneously

**Table 3. Effect of Citrus Juices and Silymarin on Serum (ALT), (AST), (ALP), NO, and GSH in Paracetamol-Induced Hepatotoxicity in Rats<sup>a</sup>**

groups	ALT (U/L)			AST (U/L)			ALP (U/L)			NO ( $\mu$ mol/g tissue)			GSH ( $\mu$ mol/g tissue)		
	mean $\pm$ SD	% change	potency	mean $\pm$ SD	% change	potency	mean $\pm$ SD	% change	potency	mean $\pm$ SD	% change	potency	mean $\pm$ SD	% change	potency
normal control	32.36 $\pm$ 0.82		100.00	53.43 $\pm$ 1.21		100.00	116.42 $\pm$ 3.72		100.00	19.31 $\pm$ 0.81		100.00	8.67 $\pm$ 0.43		100.00
paracetamol toxic dose	149.57 $\pm$ 4.31*	362.21 <sup>n</sup>		237.68 $\pm$ 6.42*	344.84 <sup>n</sup>		321.43 $\pm$ 8.97*	176.10 <sup>n</sup>		63.37 $\pm$ 1.42*	228.17 <sup>n</sup>		3.21 $\pm$ 0.12*	$-62.98$ <sup>n</sup>	
paracetamol + Silymarin	48.72 $\pm$ 1.93**	$-67.43$ <sup>p</sup>	100.00	67.39 $\pm$ 3.27**	$-71.65$ <sup>p</sup>	100.00	131.37 $\pm$ 5.21**	$-59.13$ <sup>p</sup>	100.00	21.13 $\pm$ 0.73	$-66.66$ <sup>p</sup>	100.00	7.86 $\pm$ 0.34@	144.86 <sup>p</sup>	100
paracetamol + OP	69.82 $\pm$ 2.36**	$-53.32$ <sup>p</sup>	79.08	133.26 $\pm$ 4.82**	$-43.93$ <sup>p</sup>	61.32	169.28 $\pm$ 5.73**	$-47.34$ <sup>p</sup>	80.05	36.92 $\pm$ 0.92**	$-41.74$ <sup>p</sup>	62.62	6.12 $\pm$ 0.31**	90.65 <sup>p</sup>	62.58
paracetamol + MP	97.46 $\pm$ 3.23**	$-34.84$ <sup>p</sup>	51.67	151.34 $\pm$ 6.29**	$-36.33$ <sup>p</sup>	50.70	185.56 $\pm$ 7.48**	$-42.27$ <sup>p</sup>	71.49	41.32 $\pm$ 1.27**	$-34.80$ <sup>p</sup>	52.20	5.41 $\pm$ 0.26**	68.54 <sup>p</sup>	47.31
paracetamol + GP	74.83 $\pm$ 2.93**	$-49.97$ <sup>p</sup>	74.11	148.16 $\pm$ 5.63**	$-37.66$ <sup>p</sup>	52.57	177.34 $\pm$ 6.34**	$-44.83$ <sup>p</sup>	75.81	39.21 $\pm$ 1.26**	$-38.13$ <sup>p</sup>	57.20	5.73 $\pm$ 0.23**	78.50 <sup>p</sup>	54.19
paracetamol + KF	80.84 $\pm$ 3.11**	$-45.95$ <sup>p</sup>	68.15	155.27 $\pm$ 5.93**	$-34.67$ <sup>p</sup>	48.39	191.32 $\pm$ 6.84**	$-40.48$ <sup>p</sup>	68.46	43.63 $\pm$ 1.98**	$-31.15$ <sup>p</sup>	46.73	5.27 $\pm$ 0.24**	64.17 <sup>p</sup>	44.30

<sup>a</sup>All data are represented as mean  $\pm$  S.E. serum alanine aminotransferase (ALT), aspartate aminotransferase (AST), alkaline phosphatase (ALP), nitric oxide (NO), and reduced glutathione (GSH). Normal control; saline only (1 mL), paracetamol toxic dose; 1725 mg/kg, b.wt., silymarin; 100 mg/kg, b.wt., juices; 3 mL/rat. OP; pineapple orange pulp juice, MP; Murcott mandarin pulp juice, GP; red grapefruit pulp juice, KF; oval kumquat whole fruit juice. \* Statistically significant difference compared to the control group at  $P < 0.05$ . \*\* Statistically significant difference compared to the paracetamol group at  $P < 0.05$ . (+) represents the percentage of increase and (−) represents the percentage of decrease in each value when compared to the normal control (n) or paracetamol group (p).

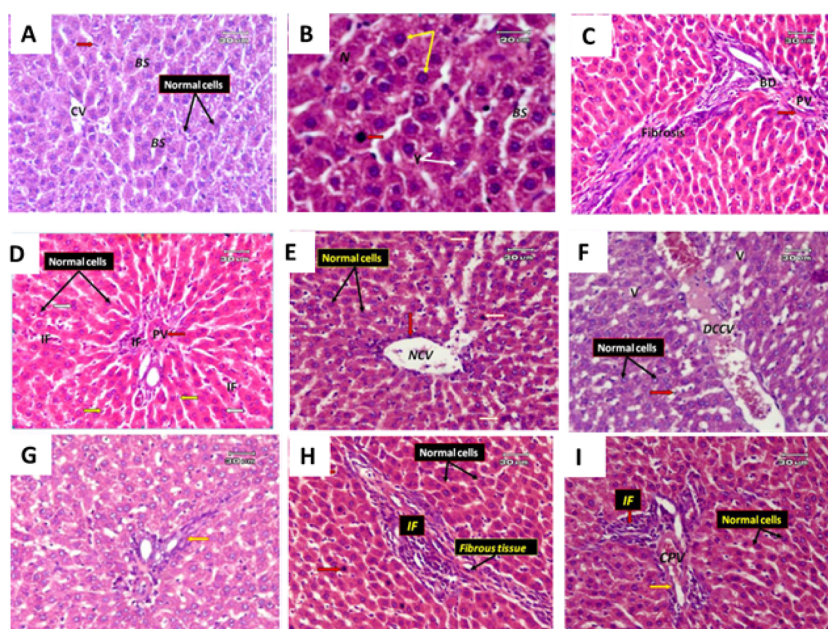


**Figure 3.** Reports the histopathological sections of different groups. (A) Normal rats ( $x = 30 \mu\text{m}$ ), (B,C) paracetamol-treated rats in toxic dose ( $x = 20, 30 \mu\text{m}$ ), (D) paracetamol-treated rats + silymarin ( $x = 30 \mu\text{m}$ ), (E) paracetamol-treated rats + OP (pineapple orange pulp juice) ( $x = 30 \mu\text{m}$ ), (F,G) paracetamol-treated rats + MP (Murcott mandarin pulp juice) ( $x = 30 \mu\text{m}$ ), (H) paracetamol-treated rats + GP (red grapefruit pulp juice) ( $x = 30 \mu\text{m}$ ), and (I) paracetamol-treated rats + FK (Oval kumquat whole fruit juice) ( $x = 30 \mu\text{m}$ ).

administered with citrus juices, some measured parameters were apparently restored to levels with no significant difference to the reference group (silymarin group). Noteworthy, in all measurements, OP juice showed the highest potency in restoring the liver parameters (ALT, AST, ALP, NO, and GSH) to normal values after paracetamol-induced hepatotoxicity, with the potency of 79.08, 61.32, 80.05, 62.62, and 62.58%, compared to the reference drug, respectively, where MP, GP, and KF showed % potency calculated to reference group values ranging from 51.67–74.11, 48.39–52.57, 68.46–75.81, 46.73–57.2, and 44.3–54.19% as ALT, AST, ALP, NO, and GSH levels, respectively.

Moreover, the histopathological sections of different groups are illustrated in Figure 3. The control group revealed normal hepatic features; the liver was observed to be composed of ill-defined hexagonal classic lobules; the hepatic lobules were organized in cords radiating from the central veins, appeared to be made of hepatocytes, and were separated by blood sinusoids. The blood sinusoids were lined by Kupffer cells and endothelial cells (Figure 3A). Furthermore, the histopathological changes of liver tissues treated with paracetamol overdose only showed signs of degeneration in hepatocytes in the form of pyknosis and karyolysis. In contrast, others showed peripheral chromatin clumping and pericentral necrosis. Bile duct proliferation and a thickened portal vein vascular wall indicate fibrosis within the portal area. The inflammation was observed primarily around the fibrous tissue and bile duct proliferation (Figure 3B,C). Histological slides from rats treated with paracetamol and silymarin revealed that the hepatic cells appeared normal despite having a thickened portal vein vascular wall and few inflammatory cells around the portal tract and in the blood sinusoids. Some binucleated and activated Kupffer cells are still present (Figure 3D). In addition, the histological sections in rats that were treated with paracetamol and OP juice exhibited some enhancement in the pathological alterations induced by paracetamol overdose, and examination of liver tissues showed

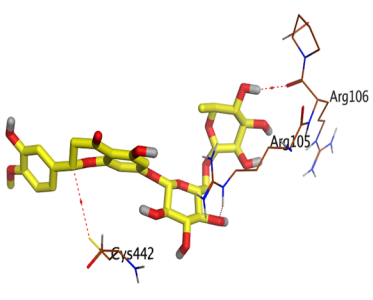
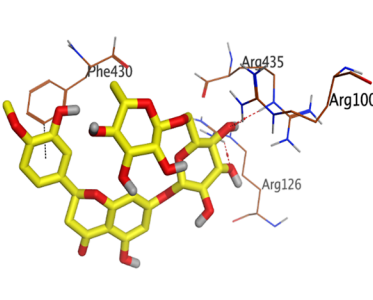
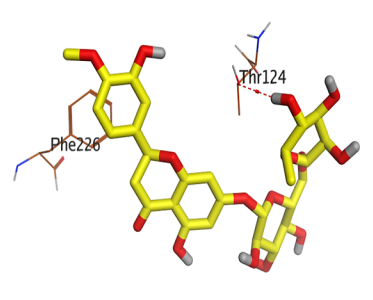
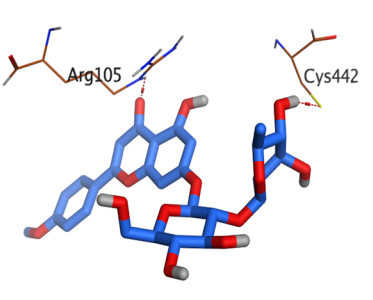
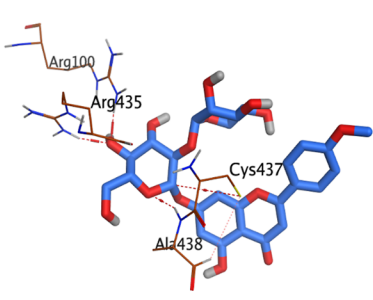
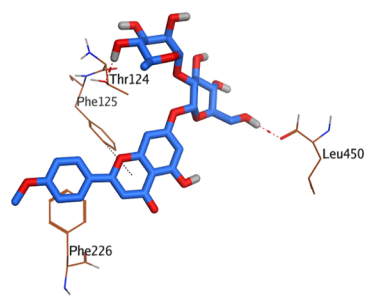
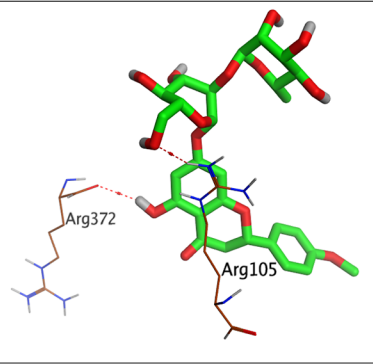
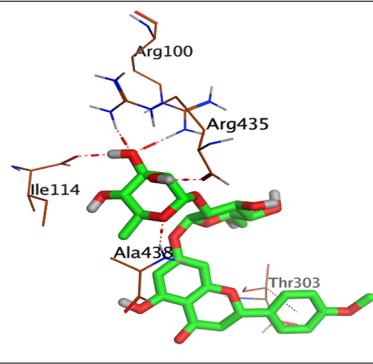
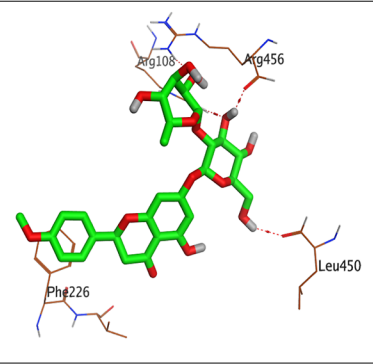
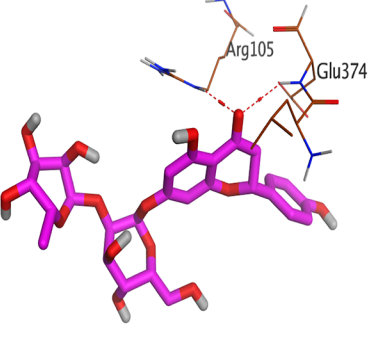
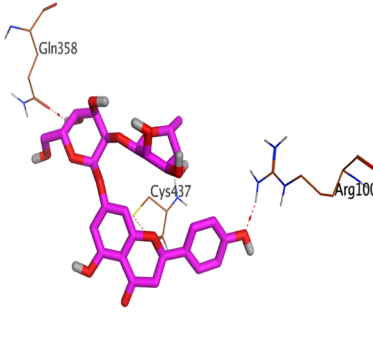
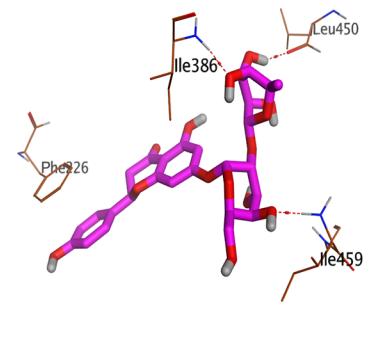
the nuclei appeared nearly normal, indicating the juice's ability to reverse the paracetamol-induced intoxication in liver tissues. However, some inflammatory cells around the normal central vein and some dark small nuclei were seen (Figure 3E). The liver section of the rats treated with paracetamol and MP juice showed that liver tissues still suffered from pathological changes in the form of hepatocytes with vacuolated cytoplasm, dilated, vacuolated, congested central veins, and dilated blood sinusoids. Early fibrosis was also seen around the portal vein. Some hepatocytes appeared nearly normal (Figure 3F,G). When rats were administered paracetamol and GP juice, some hepatocytes appeared normal, although there were pyknotic nuclei with inflammatory cell infiltration around the portal tract and bridging necrosis with early fibrosis still present (Figure 3H). Finally, light microscopic examination in the liver of rats treated with paracetamol and KF juice showed a reduction of pathological changes in the form of most nuclei appearing nearly normal. However, some changes were still present in the form of inflammatory cell infiltration around the congested portal tract with early fibrosis (Figure 3I).

The rats received paracetamol at the toxic dose (1725 mg/kg, oral); the protective groups administered silymarin at a dose of 100 mg/kg or juice at a dose of 3 mL/rat, normal group; saline only (1 mL).

BD; bile duct proliferation, BS; blood sinusoids, CPV; congested portal vein, CV; central vein, DCCV; dilated congested central vein, IF; cell infiltration, N; necrosis, NCV; normal central vein, PV; portal vein, V; vacuolar degeneration, Y; karyolysis.

$$\begin{aligned} & \% \text{ change of the tested sample and silymarin} \\ &= \frac{\text{mean of the tested sample} - \text{mean of paracetamol}}{\text{mean of paracetamol}} \\ & \times 100 \end{aligned}$$

**Table 4. 3D Binding Interactions of Hesperidin, Fortunellin, Poncirin, and Naringin within the Active Pockets of Cytochrome P450 Isoforms (CYP3A4, CYP2E1, and CYP1A2), Respectively**

Compound	Target receptor		
	CYP3A4	CYP2E1	CYP1A2
Hesperidin			
Fortunellin			
Poncirin			
Naringin			

% change of paracetamol

$$= \frac{\text{mean of paracetamol} - \text{mean of normal control}}{\text{mean of normal control}} \times 100$$

**2.6. Molecular Docking Studies.** Hesperidin, hesperetin, phloretin 3',5'-Di-C-glucoside, fortunellin, poncirin, nobiletin, apigenin-6,8-digalactoside, 6',7'-dihydroxybergamottin, naringenin, and naringin as the major identified metabolites from

citrus juices were docked against the active pockets of cytochrome P450 isoforms (CYP3A4, CYP2E1, and CYP1A2). The most promising compounds in the three docking processes were hesperidin, fortunellin, poncirin, and naringin. Therefore, these compounds were selected for further investigation.

Regarding the binding pocket of the CYP3A4 isoform (Table 4), the docked co-crystallized inhibitor got a binding score of  $-10.57$  kcal/mol (rmsd = 1.10 Å) with the formation of H-

bonds with Arg375, Arg105, and Arg106, a coordinate bond with Cys442, and a pi-H-bond with Phe100. However, hesperidin, fortunellin, poncirin, and naringin binding scores were recorded to be  $-9.50$ ,  $-9.06$ ,  $-9.68$ , and  $-9.24$  kcal/mol at rmsd values of 1.55, 1.64, 1.60, and 1.56 Å, respectively. Hesperidin formed three H-bonds with Arg105, Arg106, and Cys442. Also, fortunellin bound both Arg105 and Cys442 with two H-bonds. However, poncirin and naringin formed two H-bonds with (Arg372 and Arg105) and (Glu374 and Arg105), respectively.

However, visualizing the binding pocket of the CYP2E1 isoform (Table 4), the docked co-crystallized inhibitor achieved a binding score of  $-4.40$  kcal/mol (rmsd = 1.66 Å) with the formation of H-bonds with Arg435, Arg100, Arg126, and His370, a coordinate bond with Cys437, and pi-H-bonds with Ala438 and Thr303. Besides, hesperidin, fortunellin, poncirin, and naringin binding scores were found to be  $-12.78$ ,  $-11.98$ ,  $-10.48$ , and  $-11.56$  kcal/mol at rmsd values of 1.73, 1.17, 1.29, and 1.34 Å, respectively. Hesperidin stabilized by forming three H-bonds with Arg435, Arg100, and Arg126, and a pi-H interaction with Phe430. Moreover, fortunellin showed four H-bonds with Arg435, Arg100, Cys437, and Ala438. Furthermore, poncirin was clear to bind Arg435, Arg100, Ile114, Ala438, and Thr303 with five H-bonds. Finally, naringin bound Arg100, Cys437, and Gln358 with three H-bonds.

Concerning the binding pocket of the CYP1A2 isoform (Table 4), the docked co-crystallized inhibitor got a binding score of  $-8.52$  kcal/mol (rmsd = 1.63 Å) with the formation of a pi-H-bond with Phe226. However, hesperidin, fortunellin, poncirin, and naringin binding scores were recorded to be  $-12.53$ ,  $-12.61$ ,  $-12.73$ , and  $-11.56$  kcal/mol at rmsd values of 1.73, 1.38, 1.76, and 1.66 Å, respectively. Hesperidin formed one H-bond with Thr124 and a pi-pi bond with Phe226. Fortunellin showed the formation of two H-bonds with Thr124 and Leu450, one pi-H-bond with Phe125, and one pi-pi interaction with Phe226. However, poncirin formed three H-bonds with Arg108, Arg456, and Leu450, besides a pi-pi bond with Phe226. On the other side, Naringin formed three H-bonds with Ile386, Ile459, and Leu450 and a pi-pi interaction with Phe226.

Based on the above findings, we can infer that the examined candidates have superior inhibitory potentials based on their promising binding scores, which outperformed those of the co-crystallized ligands in CYP2E1 and CYP1A2 target receptors. The close binding modes to the co-crystallized inhibitors also indicated the proposed inhibitory potentials.

### 3. DISCUSSION

Medical practitioners and other health professionals should increase patient awareness about possible adverse food/drug-herb interactions and support patients in minimizing the risk of these interactions. As an analgesic and antipyretic, paracetamol is extensively used. It was used repeatedly during the COVID-19 pandemic in high doses and sometimes reached the risk limit of paracetamol toxicity.<sup>2</sup> Paracetamol is safe at prescribed doses, while overdose or misuse of paracetamol can be a reason for acute liver failure and even irreversible liver injury requiring liver transplantation.<sup>55</sup>

After a paracetamol overdose, the main metabolic pathways of sulfation and glucuronidation become saturated, and the excess paracetamol is bioactivated by cytochrome P450 isoenzymes the hepatotoxic NAPQI.<sup>9</sup> N-acetyl cysteine is considered the main antidote for the treatment of paracetamol overdose cases by converting NAPQI into non-toxic conjugates of mercaptate and

cysteine.<sup>10</sup> On the other hand, N-acetylcysteine does not stop the further production of these hepatotoxic metabolites,<sup>56</sup> and the only route to prevent more NAPQI formation is searching for cytochrome P450 enzyme inhibitors to block this hepatotoxic conversion pathway. Grapefruit-drug interaction is a common major type of interaction through potent inhibition of cytochrome liver enzymes such as CYP3A4.<sup>57</sup> In 2018, the FDA warned against this type of interaction and published a warning letter titled "grapefruit juice and some drugs do not mix."<sup>58,59</sup>

This study screened out different species of common citrus fruits in Egypt for the possible occurrence of this type of interaction compared to grapefruit, which is well known for its CYP450 interactions assisted by their powerful antioxidant activity and hepatoprotective actions. Additionally, the chemical profiles of the investigated samples were studied to relate the activity with detected metabolites.

The phytochemicals of citrus plants are diverse and vary with their species, origin, and different tissues.<sup>60,61</sup> The chemical profiles of the investigated species were tentatively characterized by UPLC-MS/MS, which is considered as one of the highly robust analytical techniques, where pineapple, sweet orange, and Murcott mandarin in Egypt did not receive sufficient chemical investigation. Metabolites were tentatively identified by comparing the accurate mass and fragmentation pattern with metabolites previously reported in the literature as well as databases using Sirius<sup>62</sup> and GNPS.<sup>36</sup> As a result, twelve juices were examined using ESI-MS in both positive and negative ion modes, resulting in the identification of about 40 metabolites from various phytochemical classes.

The plant phenolic content is frequently present in leaves, fruits, vegetables, nuts, seeds, etc. The consumption of fruit juices is highly valuable because of their ascorbic acid content and other phenolic compounds and carotenoids.<sup>17</sup> They serve as singlet oxygen quenchers, hydrogen donors, reducing agents, and metal chelators.<sup>63</sup> In this context, citrus juices (Rutaceae), the most popular fruits, are known to protect against oxidative stress due to their phenolic content.<sup>63,64</sup> The antioxidant capacity of citrus fruit juices is directly linked to total phenolic, carotenoids, and vitamin C content. Flavonoids, such as hesperidin, naringin, and naringenin, are important in reducing ROS.<sup>61,65</sup> Thus, we could correlate the total phenolic results and metabolite profile with the observed antioxidant capacities in this section. Remarkably, among the juice samples, OP exhibited the greatest antioxidant potential in all measured *in vitro* assays, where the estimated phenolic content concurred with the promising antioxidant activities. Furthermore, the profiles of the four juices showed the presence of approximately 25 flavonoids as well as 5 phenolic acids and glycosides, all of which were responsible for the detected significant antioxidant activity.<sup>66</sup>

From the literature survey, liver damage results in cellular enzymes seeping into the bloodstream that could be quantified in the serum. Consequently, serum ALT, AST, and ALP values are commonly used as indicators of the severity of liver disease.<sup>67</sup> Our study illustrated liver function parameters obtained 48 h after oral administration of paracetamol overdose alone and in combination with silymarin or citrus juices. Therefore, after co-administration of paracetamol with citrus juices, all *in vivo* biochemical parameters were significantly enhanced, evidenced by a normal histopathological pattern of hepatocytes. Besides, all tested citrus juices revealed promising *in vivo* antioxidant action, which may synergistically aid in restoring normal liver function after toxic invaders. However, the main suggested mechanism

behind this hepatoprotective action may refer to the inhibitory effect of citrus juices on some cytochrome P450 isoforms.

Molecular docking is considered one of the most promising computational chemistry tools to investigate the proposed mechanism of action for a particular drug or describe the binding interaction pattern for a known mechanism of action.<sup>68</sup> Although previously reported grapefruit interactions with cytochrome P450 had been mediated through furanocoumarins,<sup>55,69,70</sup> our UPLC results revealed different chemical classes that may play the same inhibitory role of furanocoumarins, where, these results were clarified and supported by a molecular docking study. The previous *in silico* studies demonstrated that several dietary flavonoid compounds, including quercetin, naringenin, naringin, and rutin, have the ability to associate with cytochromes P450 as the CYP1A2 isoform.<sup>71</sup> Interestingly, this current molecular docking study highlighted the proposed interaction of major constituents in juices with the main three CYP isoforms that are mainly involved in NAPQI formation, showing superior affinity exceeding the co-crystallized ligands in CYP2E1 and CYP1A2. Moreover, it was the first time to investigate the inhibitory action of fortunellin and poncirin on those CYP enzymes *in silico*.

Outstandingly, this study introduced insights into the efficient role of citrus juices in the management of liver damage induced after an overdose of paracetamol. This supported the probability of a direct inhibitory effect of the tested samples on cytochrome P450 enzymes, which consequently decreased the level of toxic metabolites. The best way to avoid hepatotoxicity is to ensure that hospitalized patients take paracetamol along with the antidote (enzyme inhibitor, citrus juice), so this study offered a unique, safe, and cheap antidote to the hazards of paracetamol hepatotoxicity. Therefore, this study tamed food/drug–herb interactions from a risk to a source of benefit.

#### 4. CONCLUSIONS AND FUTURE PERSPECTIVES

Flavonoids, phenolic acids, and coumarins were detected by UPLC-MS/MS and estimated by Folin–Ciocalteu, where chemometric analysis revealed that eight metabolites represented the crucial discriminatory metabolites. The *in vivo* study suggested that dietary supplementation with citrus juice may be a novel protocol for the protection and treatment of paracetamol-induced liver toxicity. Furthermore, molecular docking studies proposed the superior inhibitory potentials of the examined candidates according to their promising binding scores, which surpassed those of co-crystallized ligands in CYP2E1 and CYP1A2 target receptors. In addition, the close binding modes to the co-crystallized inhibitors suggested the proposed inhibitory potentials that would significantly decrease paracetamol-induced liver injury and death. Conclusively, the co-administration of citrus juices as an enzyme inhibitor with a toxic dose of paracetamol reduced the risk of paracetamol-induced hepatotoxicity in rats. Finally, the study switched food/drug–herb interaction from a source of risk to a source of benefit. Moreover, clinical practice and future scientific studies such as bioavailability, pharmacokinetic interactions, and pharmacodynamics of the major compounds of citrus are in demand to support the prediction of molecular docking simulations.

#### 5. MATERIALS AND METHODS

**5.1. Plant Material.** The fruits of *Citrus sinensis* L. Osbeck *var.* Pineapple (pineapple sweet orange) (O), *Citrus reticulata*

Blanco × *Citrus sinensis* L. Osbeck (Murcott mandarin) (M), *Citrus paradisi* Macfadyen *var.* Ruby Red (red grapefruit) (G), and *F. margarita* Swingle (oval kumquat) (K) were collected in the mid-season (February 2019). The plant was kindly identified by Professor Dr. Gamal Elashmanty, Head of Citrus Research Department, Citrus Research Department, Horticultural Research Institute, Agricultural Research Centre (El-Gamaa St. 9, Orman, Giza, Egypt). Voucher specimen nos. (28.12.22 I, 28.12.22 II, 28.12.22 III, and 29.12.22, respectively) are kept at the herbarium of the Department of Pharmacognosy, Faculty of Pharmacy, Cairo University, Egypt.

**5.2. Chemicals and Instruments.** A microplate reader (Tecan, USA) was used for total phenolic. Where, a plate reader (FluoStar Omega, Germany) was used in antioxidant assays. 96-Well Microplate for ELISA Assay, Flat bottom, 350  $\mu$ L/well working volume was used. Trolox, Methanol-HPLC grade, 2,4,6-Tris(2-pyridyl)-1,3,5-triazine (TPTZ), 2'-Azobis(2-aminopropane) dihydrochloride (AAPH), 2,2'-azino-bis(3-ethylbenzthiazoline-6-sulphonic acid (ABTS), and Folin–Ciocalteu's phenol reagent were obtained from Aldrich Chemicals (St. Louis, MO, USA).  $\text{Na}_2\text{CO}_3$ , sodium phosphate, hydrochloric acid, and ferric chloride were purchased from El-Nasr Company for Pharmaceutical Chemicals, Egypt.

**5.3. Preparation of Samples.** The samples that were subjected to UPLC-MS/MS and multivariate analysis consisted of 12 citrus juices prepared in the laboratory in three forms per species: juice from the pulp (P) (using a juice squeezer), pulp and albedo, and whole fruit (F) (using a blender). Thus, the samples of pineapple sweet orange (O) are OP, OPA, and OF, and those of Murcott mandarin (M) are MP, MPA, and MF, while those of red grapefruit (G) are GP, GPA, and GF, and finally, the samples of oval kumquat (K) are KP, KPA, and KF. However, only four juices of the previously mentioned ones were subjected to total phenolic, *in vitro*, and *in vivo* biological assays. Those four forms of juices are the most administered in daily life. Thus, OP, MP, and GP were selected in addition to KF, which is eaten whole with its peel.<sup>72</sup>

**5.4. UHPLC-QTOF-MS/MS Profiling.** UHPLC was run on an Agilent LC-MS system composed of an Agilent 1290 Infinity II UHPLC coupled to an Agilent 6545 ESI-Q-TOF-MS in both negative and positive modes. Aliquots (1  $\mu$ L) of citrus juices (1 mg/mL in MeOH) were analyzed following the method previously described.<sup>73</sup>

**5.5. Chemometric Analysis (Metabolic Discrimination of Citrus Fruits Using LC/MS Analyses Coupled with Chemometrics).** Metabolic discrimination of citrus species was done depending upon qualitative and quantitative data gathered from LC/MS analyses of the juices obtained from different parts of their fruits and coupled with multivariate data analysis. This was done *via* PCA and HCA as unsupervised pattern recognition models. CAMO's Unscrambler X 10.4 software (Computer-Aided Modeling, As, Norway) was used to accomplish both models as reported before.<sup>74,75</sup>

**5.6. Total Phenolic Content.** The total phenolic content was estimated using the Folin–Ciocalteu method, described by the previously described method.<sup>76</sup> Data are expressed as means  $\pm$  SD.

**5.7. In Vitro Assessment of Antioxidant Capacity.** The free radical scavenging activity of the samples was determined using 2,2'-azino-bis(3-ethylbenzthiazoline-6-sulfonic acid (ABTS) according to the published method.<sup>77</sup> In order to determine the reducing power activity, the ferric-reducing antioxidant power (FARP) assay was used.<sup>78</sup> Finally, the

peroxide radical quenching activity using the oxygen radical absorbance capacity (ORAC) assay.<sup>79</sup> Antioxidant capacities were expressed in micromoles of Trolox equivalent per mg sample ( $\mu\text{M TE}/\text{mg sample}$ ) and are represented as means ( $n = 3$ )  $\pm$  SD.

### 5.8. In Vivo Assessment of the Interactions of Citrus Juices in Case of Paracetamol Overdose-Induced Hepatotoxicity.

**5.8.1. Animal Care.** Adult albino rats (male, 130–150 g) were obtained from the National Research Center' Animal House in Cairo. They were kept under the same hygienic condition, they were fed on a standard laboratory diet, and water was supplied *ad libitum*. The experimental design was approved by the Institutional research ethics committee (MP-3089) at the Faculty of Pharmacy, Cairo University, Egypt.

#### 5.8.2. Drugs and Biochemical Kits.

- PAR tablets (500 mg of pure drug per tablet) were purchased from Chemical Industries Development Company "CID", A.R.E. Silymarin (SIL) sachets were obtained from South Egypt Industries Company "SED-ICO", A.R.E.
- Kits for determination of ALT, AST, ALP, NO, and GSH were obtained from Biodiagnostic Co. Egypt (Ad Doqi, El Omraniya, Giza Governorate).

**5.8.3. Experimental Design.** Seven groups of six rodents ( $n = 6$ ) each were formed by randomly dividing the rats into groups. PAR and SIL were dissolved in 1 mL of normal saline. The first group (GP I) served as normal control and received normal saline (1 mL) orally. The second group (GP II) was treated with a single oral toxic dose of paracetamol (1725 mg/kg b.wt.).<sup>9</sup> The other groups (GP III–VII) were separately treated once with oral doses of silymarin (100 mg/kg b.wt.),<sup>80</sup> or OP, MP, GP, and KF (3 mL/rat)<sup>9</sup> and co-administered with the toxic dose of paracetamol.

**5.8.4. Biochemical Analysis.** After 48 h of administration, rats were anesthetized using thiopental (50 mg/kg, IP). Blood samples were collected from retro-orbital sinus, then centrifuged to separate serum, and kept at  $-80\text{ }^{\circ}\text{C}$  for the determination of biochemical parameters in serum, *viz.*, ALT,<sup>81</sup> AST,<sup>81</sup> and ALP.<sup>82</sup>

Then, the livers were excised and divided into two parts. One of them was washed with ice-cold saline solution (0.9% NaCl), weighed, and then homogenized with 0.1 M phosphate buffer saline at pH 7.4 to give a final concentration of 10% w/v for more biochemical measurement in tissues; NO (nitric oxide),<sup>83</sup> and GSH (glutathione reductase).<sup>84</sup>

**5.8.5. Histopathological Studies.** The second piece of liver underwent a saline wash before being rapidly fixed in 10% formalin. The samples were then analyzed using conventional histopathological methods. Hematoxylin and eosin (H&E) was used to prepare sections of 6  $\mu\text{m}$  thickness, which were then inspected under a microscope and captured on camera.

**5.8.6. Statistical Analysis.** All data are expressed as mean  $\pm$  SE and analyzed by one-way ANOVA and Duncan's multiple-range test compared the means of different groups.  $P < 0.05$  was considered statistically significant.

**5.9. Molecular Docking Studies.** The major identified metabolites from citrus juices were docked against the active pockets of cytochrome P450 isoforms (CYP3A4, CYP2E1, and CYP1A2) in three different docking processes to investigate their inhibitory potentials. Therefore, hesperidin, hesperetin, phloretin 3',5'-Di-C-glucoside, fortunellin, poncirin, nobiletin, apigenin-6,8-digalactoside, 6',7'-dihydroxybergamottin, narin-

genin, and naringin were sketched in ChemDraw. After, the chemical structures of the aforementioned compounds were copied and pasted into the MOE<sup>85,86</sup> working window individually. Each compound was corrected for partial charges and energy-minimized to improve its stability.<sup>87</sup> The prepared compounds and the co-crystallized inhibitor in each target receptor were inserted in a single database. Besides, the target protein structures of cytochrome P450 isoforms (CYP3A4, CYP2E1, and CYP1A2) were obtained from the PDB website (accessed on 1/3/2023) (<https://www.rcsb.org/structure/8EWD>, <https://www.rcsb.org/structure/3E6I>, and <https://www.rcsb.org/structure/2H14>, respectively). Each protein was opened using the MOE, corrected, 3D hydrogenated, and energy-minimized, as discussed before.<sup>88</sup> Three general docking processes with the default program specifications<sup>89</sup> were performed by inserting the appropriate database for each target receptor. The superior compounds with the best docking scores and root mean square deviation (rmsd) values<sup>90</sup> were selected. Furthermore, three validation processes were done by redocking the co-crystallized inhibitor in each target receptor within its binding pocket. The valid performance was confirmed by finding low rmsd values ( $<2\text{ \AA}$ ) in each case.<sup>91</sup>

## AUTHOR INFORMATION

### Corresponding Author

Aya S. Shalaby – Pharmacognosy Department, Faculty of Pharmacy, Cairo University, Cairo 11562, Egypt;  
[orcid.org/0009-0006-0919-8035](https://orcid.org/0009-0006-0919-8035); Email: [aya.saifeldin@pharma.cu.edu.eg](mailto:aya.saifeldin@pharma.cu.edu.eg)

### Authors

- Hanaa H. Eid – Pharmacognosy Department, Faculty of Pharmacy, Cairo University, Cairo 11562, Egypt
- Riham A. El-Shiekh – Pharmacognosy Department, Faculty of Pharmacy, Cairo University, Cairo 11562, Egypt;  
[orcid.org/0000-0002-3179-3352](https://orcid.org/0000-0002-3179-3352)
- Osama G. Mohamed – Pharmacognosy Department, Faculty of Pharmacy, Cairo University, Cairo 11562, Egypt; Natural Products Discovery Core, Life Sciences Institute, University of Michigan, Ann Arbor, Michigan 48109, United States;  
[orcid.org/0000-0003-3216-6948](https://orcid.org/0000-0003-3216-6948)
- Ashootosh Tripathi – Natural Products Discovery Core, Life Sciences Institute, University of Michigan, Ann Arbor, Michigan 48109, United States; Department of Medicinal Chemistry, College of Pharmacy, University of Michigan, Ann Arbor, Michigan 48109, United States; [orcid.org/0000-0003-2297-8088](https://orcid.org/0000-0003-2297-8088)
- Ahmed A. Al-Karmalawy – Pharmaceutical Chemistry Department, Faculty of Pharmacy, Ahram Canadian University, Giza 12566, Egypt; [orcid.org/0000-0002-8173-6073](https://orcid.org/0000-0002-8173-6073)
- Amany A. Sleem – Pharmacology Department, National Research Centre, Cairo 12622, Egypt
- Fatma Adly Morsy – Pathology Department, National Research Centre, Cairo 12622, Egypt
- Khaled M. Ibrahim – Pharmacognosy Department, Faculty of Pharmacy, Cairo University, Cairo 11562, Egypt
- Soad H. Tadros – Pharmacognosy Department, Faculty of Pharmacy, Cairo University, Cairo 11562, Egypt
- Fadia S. Youssef – Department of Pharmacognosy, Faculty of Pharmacy, Ain-Shams University, Cairo 11566, Egypt;  
[orcid.org/0000-0002-5871-2639](https://orcid.org/0000-0002-5871-2639)

Complete contact information is available at:

<https://pubs.acs.org/10.1021/acsomega.3c03100>

## Notes

The authors declare no competing financial interest.

## REFERENCES

- (1) Saccomano, S. J. Acute acetaminophen toxicity in adults. *Nursing2020 Critical Care* **2019**, *44*, 42–47.
- (2) Mostafa, E. M.; Tawfik, A. M.; Abd-Elrahman, K. M. Egyptian perspectives on potential risk of paracetamol/acetaminophen-induced toxicities: Lessons learnt during COVID-19 pandemic. *Toxicol Rep.* **2022**, *9*, 541–548.
- (3) Yoon, E.; Babar, A.; Choudhary, M.; Kutner, M.; Pyrsopoulos, N. Acetaminophen-induced hepatotoxicity: a comprehensive update. *J. Clin. Transl. Hepatol.* **2016**, *4*, 131.
- (4) Abdelhamid, W. Evaluation of severity of poisoning exposures among patients presented to Poison Control Center, Ain Shams University Hospitals, Egypt during 2019. *Ain Shams journal of forensic medicine and clinical toxicology* **2021**, *36*, 106–122.
- (5) WHO. Updated: WHO Now Doesn't Recommend Avoiding Ibuprofen For COVID-19 Symptoms, 2020. <https://www.sciencealert.com/who-recommends-to-avoid-taking-ibuprofen-for-covid-19-symptoms>. (accessed on October 16, 2020).
- (6) Enners, S.; Gradl, G.; Kieble, M.; Böhm, M.; Laufs, U.; Schulz, M. Utilization of drugs with reports on potential efficacy or harm on COVID-19 before, during, and after the first pandemic wave. *Pharmacoepidemiol. Drug Saf.* **2021**, *30*, 1493–1503.
- (7) Ibrahimagić, O. C.; Ercegović, Z.; Vujadinović, A.; Kunić, S. Comment on an article: "Medications in COVID-19 patients: summarizing the current literature from an orthopaedic perspective". *Int. Orthop.* **2020**, *44*, 2811–2812.
- (8) Sestili, P.; Fimognari, C. Paracetamol-induced glutathione consumption: is there a link with severe COVID-19 illness? *Front. Pharmacol.* **2020**, *11*, 1597.
- (9) Baleni, R.; Bekker, Z.; Walubo, A.; Du Plessis, J. B. Co-administration of fresh grape fruit juice (GFJ) and bergamottin prevented paracetamol induced hepatotoxicity after paracetamol overdose in rats. *Toxicol Rep.* **2015**, *2*, 677–684.
- (10) Bertolini, A.; Ferrari, A.; Ottani, A.; Guerzoni, S.; Tacchi, R.; Leone, S. Paracetamol: new vistas of an old drug. *CNS Drug Rev.* **2006**, *12*, 250–275.
- (11) Brown, S. A.; Axenfeld, E.; Stonesifer, E. G.; Hutson, W.; Hanish, S.; Raufman, J.-P.; Urrunaga, N. H. Current and prospective therapies for acute liver failure. *Disease-a-Month* **2018**, *64*, 493–522.
- (12) Ye, Z.; Hu, J.; Wang, J.; Liu, Y.-n.; Hu, G.-x.; Xu, R.-a. The effect of Resveratrol on the pharmacokinetic profile of tofacitinib and the underlying mechanism. *Chem.-Biol. Interact.* **2023**, *374*, 110398.
- (13) Liu, Y.-n.; Chen, J.; Wang, J.; Li, Q.; Hu, G.-x.; Cai, J.-p.; Lin, G.; Xu, R. a. Effects of drug-drug interactions and CYP3A4 variants on alectinib metabolism. *Arch. Toxicol.* **2023**, *97*, 2133–2142.
- (14) Walubo, A.; Barr, S.; Abraham, A.; Coetsee, C. The role of cytochrome-P450 inhibitors in the prevention of hepatotoxicity after paracetamol overdose in rats. *Hum. Exp. Toxicol.* **2004**, *23*, 49–54.
- (15) Lü, J.; Zhang, D.; Zhang, X.; Sa, R.; Wang, X.; Wu, H.; Lin, Z.; Zhang, B. Network Analysis of the Herb–Drug Interactions of Citrus Herbs Inspired by the "Grapefruit Juice Effect". *ACS Omega* **2022**, *7*, 35911–35923.
- (16) Kumarappan, C.; Vijayakumar, M.; Thilagam, E.; Balamurugan, M.; Thiagarajan, M.; Senthil, S.; Das, S. C.; Mandai, S. C. Protective and curative effects of polyphenolic extracts from *Ichnocarpus frutescens* leaves on experimental hepatotoxicity by carbon tetrachloride and tamoxifen. *Ann. Hepatol.* **2011**, *10*, 63–72.
- (17) Hamdan, D. I.; El-Shiekh, R. A.; El-Sayed, M. A.; Khalil, H. M.; Mousa, M. R.; Al-Gendy, A. A.; El-Shazly, A. M. Phytochemical characterization and anti-inflammatory potential of Egyptian *Murcott* mandarin cultivar waste (stem, leaves and peel). *Food Funct.* **2020**, *11*, 8214–8236.
- (18) Tala, D. S.; Gatsing, D.; Fodouop, S. P. C.; Fokunang, C.; Kengni, F.; Djimeli, M. N. In vivo anti-salmonella activity of aqueous extract of *Euphorbia prostrata* Aiton (Euphorbiaceae) and its toxicological evaluation. *Asian Pac. J. Trop. Biomed.* **2015**, *5*, 310–318.
- (19) Ameer, B.; Weintraub, R. A. Drug interactions with grapefruit juice. *Clin. Pharmacokinet.* **1997**, *33*, 103–121.
- (20) Kane, G. C.; Lipsky, J. J. Drug–grapefruit juice interactions. *Mayo Clinic Proceedings*; Elsevier, 2000; pp 933–942.
- (21) Kirby, B.; Unadkat, J. Grapefruit juice, a glass full of drug interactions? *Clin. Pharmacol. Ther.* **2007**, *81*, 631–633.
- (22) Lou, S.-N.; Ho, C.-T. Phenolic compounds and biological activities of small-size citrus: Kumquat and calamondin. *J. Food Drug Anal.* **2017**, *25*, 162–175.
- (23) Barreca, D.; Mandalari, G.; Calderaro, A.; Smeriglio, A.; Trombetta, D.; Felice, M. R.; Gattuso, G. Citrus flavones: An update on sources, biological functions, and health promoting properties. *Plants* **2020**, *9*, 288.
- (24) Son, N. T. Notes on the genus *Paramignya*: phytochemistry and biological activity. *Bull. Fac. Pharm. Cairo Univ.* **2018**, *56*, 1–10.
- (25) Ogawa, K.; Kawasaki, A.; Omura, M.; Yoshida, T.; Ikoma, Y.; Yano, M. 3', 5'-Di-C- $\beta$ -glucopyranosylphloretin, a flavonoid characteristic of the genus *Fortunella*. *Phytochemistry* **2001**, *57*, 737–742.
- (26) Edwards, D. J.; Bellevue, F.; Woster, P. M. Identification of 6', 7'-dihydroxybergamottin, a cytochrome P450 inhibitor, in grapefruit juice. *Drug Metab. Dispos.* **1996**, *24*, 1287–1290.
- (27) Matheyambath, A.; Padmanabhan, P.; Paliyath, G. *Citrus Fruits: Encyclopedia of Food and Health*; Elsevier: Amsterdam, The Netherlands, 2016.
- (28) Qing, Z.; Xu, Y.; Yu, L.; Liu, J.; Huang, X.; Tang, Z.; Cheng, P.; Zeng, J. Investigation of fragmentation behaviours of isoquinoline alkaloids by mass spectrometry combined with computational chemistry. *Sci. Rep.* **2020**, *10*, 7373.
- (29) Chiarelli, M. P.; Gross, M. L. Mechanism of cationization of sucrose by sodium in laser desorption: a study by Fourier transform mass spectrometry. *Int. J. Mass Spectrom. Ion Process.* **1987**, *78*, 37–52.
- (30) Brito, A.; Ramirez, J. E.; Areche, C.; Sepúlveda, B.; Simirgiotis, M. J. HPLC-UV-MS profiles of phenolic compounds and antioxidant activity of fruits from three citrus species consumed in Northern Chile. *Molecules* **2014**, *19*, 17400–17421.
- (31) Servillo, L.; Giovane, A.; Casale, R.; Cautela, D.; D'Onofrio, N.; Balestrieri, M. L.; Castaldo, D. Glucosylated forms of serotonin and tryptophan in green coffee beans. *LWT* **2016**, *73*, 117–122.
- (32) van de Weert, M.; Lagerwerf, F. M.; Haverkamp, J.; Heerma, W. Mass spectrometric analysis of oxidized tryptophan. *J. Mass Spectrom.* **1998**, *33*, 884–891.
- (33) Cheiran, K. P.; Raimundo, V. P.; Manfroi, V.; Anzanello, M. J.; Kahmann, A.; Rodrigues, E.; Frazzon, J. Simultaneous identification of low-molecular weight phenolic and nitrogen compounds in craft beers by HPLC-ESI-MS/MS. *Food Chem.* **2019**, *286*, 113–122.
- (34) Allegrone, G.; Pecci, Y.; Mauro, M.; Orsetti, M. Determination of Eleutherosides in Dietary Supplements by LC–MS/MS. *Chromatographia* **2013**, *76*, 41–48.
- (35) Wang, K.; Tian, J.; Li, Y.; Liu, M.; Chao, Y.; Cai, Y.; Zheng, G.; Fang, Y. Identification of components in *Citri Sarcodactylis Fructus* from different origins via UPLC-Q-Exactive Orbitrap/MS. *ACS Omega* **2021**, *6*, 17045–17057.
- (36) Leao, T. F.; Clark, C. M.; Bauermeister, A.; Elijah, E. O.; Gentry, E. C.; Husband, M.; Oliveira, M. F.; Bandeira, N.; Wang, M.; Dorrestein, P. C. Quick-start infrastructure for untargeted metabolomics analysis in GNPS. *Nat. Metabol.* **2021**, *3*, 880–882.
- (37) Shao, S.-Y.; Ting, Y.; Wang, J.; Sun, J.; Guo, X.-F. Characterization and identification of the major flavonoids in *Phyllostachys edulis* leaf extract by UPLC–QTOF–MS/MS. *Acta Chromatogr.* **2020**, *32*, 228–237.
- (38) Zhang, H. J. Profiling analysis of the seeds of *Vaccaria segetalis* (Necr.) Gracke by HPLC-ESI-MS. *Advanced Materials Research*; Trans Tech Publ, 2012; pp 96–98.
- (39) Carini, M.; Facino, R. M.; Aldini, G.; Calloni, M.; Colombo, L. Characterization of phenolic antioxidants from *Maté* (*Ilex Para-*

- guayensis) by liquid chromatography/mass spectrometry and liquid chromatography/tandem mass spectrometry. *Rapid Commun. Mass Spectrom.* **1998**, *12*, 1813–1819.
- (40) Mei, Z.; Zhang, R.; Zhao, Z.; Xu, X.; Chen, B.; Yang, D.; Zheng, G. Characterization of antioxidant compounds extracted from Citrus reticulata cv. Chachiensis using UPLC-Q-TOF-MS/MS, FT-IR and scanning electron microscope. *J. Pharm. Biomed. Anal.* **2021**, *192*, 113683.
- (41) Barreca, D.; Bellocco, E.; Caristi, C.; Leuzzi, U.; Gattuso, G. Kumquat (*Fortunella japonica* Swingle) juice: Flavonoid distribution and antioxidant properties. *Food Res. Int.* **2011**, *44*, 2190–2197.
- (42) Zhang, J.; Yang, J.; Duan, J.; Liang, Z.; Zhang, L.; Huo, Y.; Zhang, Y. Quantitative and qualitative analysis of flavonoids in leaves of *Adinandra nitida* by high performance liquid chromatography with UV and electrospray ionization tandem mass spectrometry detection. *Anal. Chim. Acta* **2005**, *532*, 97–104.
- (43) Ek, S.; Kartimo, H.; Mattila, S.; Tolonen, A. Characterization of phenolic compounds from lingonberry (*Vaccinium vitis-idaea*). *J. Agric. Food Chem.* **2006**, *54*, 9834–9842.
- (44) Lee, J.; Mitchell, A. E. Pharmacokinetics of quercetin absorption from apples and onions in healthy humans. *J. Agric. Food Chem.* **2012**, *60*, 3874–3881.
- (45) Dadheech, N.; Soni, S.; Srivastava, A.; Dadheech, S.; Gupta, S.; Gopurappilly, R.; Bhonde, R. R.; Gupta, S. A small molecule Swertisin from *Enicostemma littorale* differentiates NIH3T3 cells into islet-like clusters and restores Normoglycemia upon transplantation in diabetic balb/c mice. *Evid. base Compl. Alternative Med.* **2013**, *2013*, 1–20.
- (46) Hsueh, T.-P.; Tsai, T.-H. Preclinical pharmacokinetics of scoparone, geniposide and rhein in an herbal medicine using a validated LC-MS/MS method. *Molecules* **2018**, *23*, 2716.
- (47) Sadek, E. S.; Makris, D. P.; Kefalas, P. Polyphenolic composition and antioxidant characteristics of kumquat (*Fortunella margarita*) peel fractions. *Plant Foods Hum. Nutr.* **2009**, *64*, 297–302.
- (48) Spigoni, V.; Mena, P.; Fantuzzi, F.; Tassotti, M.; Brighenti, F.; Bonadonna, R. C.; Del Rio, D.; Dei Cas, A. Bioavailability of bergamot (*Citrus bergamia*) flavanones and biological activity of their circulating metabolites in human pro-angiogenic cells. *Nutrients* **2017**, *9*, 1328.
- (49) Zhao, L.; Jin, X.; Xiong, Z.; Tang, H.; Guo, H.; Ye, G.; Chen, D.; Yang, S.; Yin, Z.; Fu, H.; et al. The Antiviral Activity of Umbelliferone and Its Protective Effect against A. hydrophila-Infected Grass Carp. *Int. J. Mol. Sci.* **2022**, *23*, 11119.
- (50) Lee, S. G.; Kim, K.; Vance, T. M.; Perkins, C.; Provas, A.; Wu, S.; Qureshi, A.; Cho, E.; Chun, O. K. Development of a comprehensive analytical method for furanocoumarins in grapefruit and their metabolites in plasma and urine using UPLC-MS/MS: a preliminary study. *Int. J. Nutr. Food Sci.* **2016**, *67*, 881–887.
- (51) Zheng, G.-D.; Zhou, P.; Yang, H.; Li, Y.-s.; Li, P.; Liu, E.-H. Rapid resolution liquid chromatography–electrospray ionisation tandem mass spectrometry method for identification of chemical constituents in Citri Reticulatae Pericarpium. *Food Chem.* **2013**, *136*, 604–611.
- (52) Abdelghffar, E. A.; El-Nashar, H. A.; Al-Mohammadi, A. G.; Eldahshan, O. A. Orange fruit (*Citrus sinensis*) peel extract attenuates chemotherapy-induced toxicity in male rats. *Food Funct.* **2021**, *12*, 9443–9455.
- (53) Yang, J.; Wang, C.; Li, N.; Wu, L.; Huang, Z.; Hu, Z.; Li, X.; Qu, Z. Phytochemicals and anti-tyrosinase activities of *Paeonia ostii* leaves and roots. *Plant Physiol. Biochem.* **2022**, *181*, 50–60.
- (54) Wang, S.; Cai, T.; Liu, H.; Yang, A.; Xing, J. Liquid chromatography-tandem mass spectrometry assay for the simultaneous determination of three major flavonoids and their glucuronidated metabolites in rats after oral administration of *Artemisia annua* L. extract at a therapeutic ultra-low dose. *J. Separ. Sci.* **2019**, *42*, 3330–3339.
- (55) Tarirai, C.; Viljoen, A. M.; Hamman, J. H. Herb–drug pharmacokinetic interactions reviewed. *Expet Opin. Drug Metabol. Toxicol.* **2010**, *6*, 1515–1538.
- (56) Bateman, D. N.; Dear, J. W. Acetylcysteine in paracetamol poisoning: a perspective of 45 years of use. *Toxicol. Res.* **2019**, *8*, 489–498.
- (57) Farkas, D.; Greenblatt, D. J. Influence of fruit juices on drug disposition: discrepancies between in vitro and clinical studies. *Expet Opin. Drug Metabol. Toxicol.* **2008**, *4*, 381–393.
- (58) Chen, M.; Zhou, S.-y.; Fabriaga, E.; Zhang, P.-h.; Zhou, Q. Food–drug interactions precipitated by fruit juices other than grapefruit juice: An update review. *J. Food Drug Anal.* **2018**, *26*, S61–S71.
- (59) Bonner, L. Grapefruit and certain medications don't mix, FDA reminds public. *Pharmacy Today* **2017**, *23*, 18.
- (60) Haraoui, N.; Allem, R.; Chaouche, T. M.; Belouazni, A. In-vitro antioxidant and antimicrobial activities of some varieties citrus grown in Algeria. *Advances in Traditional Medicine* **2020**, *20*, 23–34.
- (61) Zou, Z.; Xi, W.; Hu, Y.; Nie, C.; Zhou, Z. Antioxidant activity of Citrus fruits. *Food Chem.* **2016**, *196*, 885–896.
- (62) Dührkop, K.; Fleischauer, M.; Ludwig, M.; Aksenov, A. A.; Melnik, A. V.; Meusel, M.; Dorrestein, P. C.; Rousu, J.; Böcker, S. SIRIUS 4: a rapid tool for turning tandem mass spectra into metabolite structure information. *Nat. Methods* **2019**, *16*, 299–302.
- (63) Rekha, C.; Poornima, G.; Manasa, M.; Abhisha, V.; Devi, J. P.; Kumar, H. T. V.; Kekuda, T. R. P. Ascorbic acid, total phenol content and antioxidant activity of fresh juices of four ripe and unripe citrus fruits. *Chemical Science Transactions* **2012**, *1*, 303–310.
- (64) Zhang, H.; YANG, Y.-f.; ZHOU, Z.-q. Phenolic and flavonoid contents of mandarin (*Citrus reticulata* Blanco) fruit tissues and their antioxidant capacity as evaluated by DPPH and ABTS methods. *J. Integr. Agric.* **2018**, *17*, 256–263.
- (65) Xu, G.; Liu, D.; Chen, J.; Ye, X.; Ma, Y.; Shi, J. Juice components and antioxidant capacity of citrus varieties cultivated in China. *Food Chem.* **2008**, *106*, 545–551.
- (66) El-Shiekh, R.; Al-Mahdy, D.; Hifnawy, M.; Abdel-Sattar, E. In-vitro screening of selected traditional medicinal plants for their anti-obesity and anti-oxidant activities. *South Afr. J. Bot.* **2019**, *123*, 43–50.
- (67) Sarkar, C.; Mondal, M.; Al-Khafaji, K.; El-Kersh, D. M.; Jamaddar, S.; Ray, P.; Roy, U. K.; Afroze, M.; Moniruzzaman, M.; Khan, M.; et al. GC–MS analysis, and evaluation of protective effect of Piper chaba stem bark against paracetamol-induced liver damage in Sprague-Dawley rats: Possible defensive mechanism by targeting CYP2E1 enzyme through in silico study. *Life Sci.* **2022**, *309*, 121044.
- (68) El-Behairy, M. F.; Abd-Allah, W. H.; Khalifa, M. M.; Nafie, M. S.; Saleh, M. A.; Abdel-Maksoud, M. S.; Al-Warhi, T.; Eldehna, W. M.; Al-Karmalawy, A. A. Design and synthesis of novel rigid dibenzo[b,f]-azepines through ring closure technique as promising anticancer candidates against leukaemia and acting as selective topoisomerase II inhibitors and DNA intercalators. *J. Enzyme Inhib. Med. Chem.* **2023**, *38*, 2157825.
- (69) Jiang, T.; Cheng, T.; Li, J.; Zhou, M.; Tan, R.; Yang, X.; Wang, Y.; Li, W.; Zheng, J. Bergapto, a mechanism-based inactivator of CYP2C9. *Med. Chem. Res.* **2020**, *29*, 1230–1237.
- (70) Hung, W.-L.; Suh, J. H.; Wang, Y. Chemistry and health effects of furanocoumarins in grapefruit. *J. Food Drug Anal.* **2017**, *25*, 71–83.
- (71) Sousa, M. C.; Braga, R. C.; Cintra, B. A.; de Oliveira, V.; Andrade, C. H. In silico metabolism studies of dietary flavonoids by CYP1A2 and CYP2C9. *Food Res. Int.* **2013**, *50*, 102–110.
- (72) Sutour, S.; Luro, F.; Bradesi, P.; Casanova, J.; Tomi, F. Chemical composition of the fruit oils of five *Fortunella* species grown in the same pedoclimatic conditions in Corsica (France). *Nat. Prod. Commun.* **2016**, *11*, 1934578X1601100.
- (73) Hamed, A. A.; El-Shiekh, R. A.; Mohamed, O. G.; Aboutabl, E. A.; Fathy, F. I.; Fawzy, G. A.; Al-Taweel, A. M.; Elsayed, T. R.; Tripathi, A.; Al-Karmalawy, A. A. Cholinesterase Inhibitors from an Endophytic Fungus *Aspergillus niveus* Fv-er401: Metabolomics, Isolation and Molecular Docking. *Molecules* **2023**, *28*, 2559.
- (74) Youssef, F. S.; Labib, R. M.; Eldahshan, O. A.; Singab, A. N. B. Synergistic Hepatoprotective and Antioxidant Effect of Artichoke, Fig, Blackberry Herbal Mixture on HepG2 Cells and Their Metabolic Profiling Using NMR Coupled with Chemometrics. *Chem. Biodiversity* **2017**, *14*, No. e1700206.
- (75) Youssef, F. S.; Labib, R. M.; Sleem, A. A.; Meselhy, K. M. Discrimination of *Vitis vinifera* varieties using DNA fingerprinting and NMR coupled with chemometrics and their impact on the efficacy of

fluoxetine and indomethacin in vivo. *J. Food Process. Preserv.* **2021**, *45*, No. e15500.

(76) Attard, E. A rapid microtitre plate Folin-Ciocalteu method for the assessment of polyphenols. *Open Life Sci.* **2013**, *8*, 48–53.

(77) Arnao, M. B.; Cano, A.; Acosta, M. The hydrophilic and lipophilic contribution to total antioxidant activity. *Food Chem.* **2001**, *73*, 239–244.

(78) Benzie, I. F.; Strain, J. J. The ferric reducing ability of plasma (FRAP) as a measure of “antioxidant power”: the FRAP assay. *Anal. Biochem.* **1996**, *239*, 70–76.

(79) Liang, Z.; Cheng, L.; Zhong, G.-Y.; Liu, R. H. Antioxidant and antiproliferative activities of twenty-four *Vitis vinifera* grapes. *PLoS One* **2014**, *9*, No. e105146.

(80) Pingili, R.; Pawar, A. K.; Challa, S. R. Quercetin reduced the formation of N-acetyl-p-benzoquinoneimine, a toxic metabolite of paracetamol in rats and isolated rat hepatocytes. *Phytother Res.* **2019**, *33*, 1770–1783.

(81) Reitman, S.; Frankel, S. A colorimetric method for the determination of serum glutamic oxalacetic and glutamic pyruvic transaminases. *Am. J. Clin. Pathol.* **1957**, *28*, 56–63.

(82) Belfield, A.; Goldberg, D. Revised assay for serum phenyl phosphatase activity using 4-amino-antipyrine. *Enzyme* **1971**, *12*, 561–573.

(83) Moshage, H.; Kok, B.; Huizenga, J. R.; Jansen, P. Nitrite and nitrate determinations in plasma: a critical evaluation. *Clin. Chem.* **1995**, *41*, 892–896.

(84) Beutler, E.; Duron, O.; Kelly, B. M. Improved method for the determination of blood glutathione. *J. Lab. Clin. Med.* **1963**, *61*, 882–888.

(85) Inc, C. *Molecular Operating Environment (MOE)*; Chemical Computing Group Inc, 2016; p 1010.

(86) Elshal, M.; Eid, N.; El-Sayed, I.; El-Sayed, W.; Al-Karmalawy, A. A. Concanavalin-A Shows Synergistic Cytotoxicity with Tamoxifen via Inducing Apoptosis in Estrogen Receptor-Positive Breast Cancer: In Vitro and Molecular Docking Studies. *Pharmaceut. Sci.* **2021**, *28*, 76–85.

(87) Khattab, M.; Al-Karmalawy, A. A. Computational repurposing of benzimidazole anthelmintic drugs as potential colchicine binding site inhibitors. *Future Med. Chem.* **2021**, *13*, 1623–1638.

(88) Taher, R. F.; Al-Karmalawy, A. A.; Abd El Maksoud, A. I.; Khalil, H.; Hassan, A.; El-Khrisy, E.-D. A.; El-Kashak, W. Two new flavonoids and anticancer activity of *Hymenosporum flavum*: in vitro and molecular docking studies. *J. HerbMed Pharmacol.* **2021**, *10*, 443–458.

(89) Diab, R. T.; Abdel-Sami, Z. K.; Abdel-Aal, E. H.; Al-Karmalawy, A. A.; Abo-Dya, N. E. Design and synthesis of a new series of 3,5-disubstituted-1,2,4-oxadiazoles as potential colchicine binding site inhibitors: antiproliferative activity, molecular docking, and SAR studies. *New J. Chem.* **2021**, *45*, 21657–21669.

(90) Elebeedy, D.; Badawy, I.; Elmaaty, A. A.; Saleh, M. M.; Kandeil, A.; Ghanem, A.; Kutkat, O.; Alnajjar, R.; Abd El Maksoud, A. I.; Al-karmalawy, A. A. In vitro and computational insights revealing the potential inhibitory effect of Tanshinone IIA against influenza A virus. *Comput. Biol. Med.* **2022**, *141*, 105149.

(91) Elmaaty, A. A.; Darwish, K. M.; Chrouda, A.; Boseila, A. A.; Tantawy, M. A.; Elhady, S. S.; Shaik, A. B.; Mustafa, M.; Al-karmalawy, A. A. In Silico and In Vitro Studies for Benzimidazole Anthelmintics Repurposing as VEGFR-2 Antagonists: Novel Mebendazole-Loaded Mixed Micelles with Enhanced Dissolution and Anticancer Activity. *ACS Omega* **2022**, *7*, 875–899.